PHYSICAL REVIEW A VOLUME 50, NUMBER 3 SEPTEMBER 1994

# Relaxation, generation, and detection of Zeeman coherences in an optically pumped heavy-alkali-metal vapor

J. A. Vallés and J. M. Alvarez

*Departamento de Física Aplicada, Facultad de Ciencias, Universidad de Zaragoza, 50009 Zaragoza, Spain*

(Received 12 October 1993; revised manuscript received 4 May 1994)

The relaxation and generation of multipole orientations in a heavy-alkali-metal vapor in the presence of a weak static magnetic field are theoretically studied both for populations and for Zeeman coherences by taking into account the effects on the evolution of the atomic density matrix of the relaxation processes (by alkali-atom–buffer-gas, alkali-atom–alkali-atom with spin exchange and alkali-atom–cell-wall collisions) and of the optical pumping with any light polarization and spectral distribution. The dependence of the stationary-state multipole orientations on the pumping characteristic parameters is numerically analyzed. The detection process of these orientations is also studied.

PACS number(s): 32.80.Bx, 32.30.Bv

## I. INTRODUCTION

Optical-pumping techniques have proved to be one of the most useful methods for studying interactions between alkali-metal atoms and inert-gas molecules [1]. In a typical Zeeman optical-pumping experiment, the alkali-metal vapor is confined in a glass cell—as well as the inert gas—in the presence of a weak magnetic field. This system is excited by a resonant light in one of the alkali-metal transitions. Depending on the polarization and the spectral distribution of this light, it tends to keep the system far from its natural equilibrium state. A number of relaxation mechanisms due to the interaction of the alkali-metal atoms with their medium try to balance that pumping process.

In most of the optical pumping experiments the information about the atomic system is obtained through optical signals. In the presence of a weak magnetic field, the optical macroscopic properties shown by a pumped alkali-metal vapor depend in a direct way only on the hyperfine, dipole, and quadrupole orientations induced in such a vapor. The relaxation and generation of hyperfine and dipole orientations have been thoroughly studied by different authors. Nevertheless, the effects of the presence of the quadrupole orientation have been analyzed only recently, both theoretically [2] and experimentally [3], although those works deal only with populations and consider very particular cases. However, there are several situations where the above-mentioned theoretical treatment is obviously insufficient. For instance, if the pumping is transversal, or in those experiments in which a radiofrequency external field connects the Zeeman sublevels of the alkali-metal atom, inducing coherences between them.

In this paper a complete theoretical study of the relaxation, generation, and detection of populations and coherences in a Zeeman optical-pumping experiment is presented. In Sec. II, we calculate the expressions of the terms of the evolution equations of the atomic density-matrix components using the irreducible formalism. The normalization condition is discussed in Sec. III, and the detection process is analyzed in Sec. IV. Finally, in Sec. V several numerical results obtained from our theoretical expressions are shown.

## II. CONTRIBUTIONS TO THE EVOLUTION OF THE ATOMIC DENSITY MATRIX

Under the typical conditions of optical pumping the internal state of the atoms is generally well described by the density matrix $\rho$, which obeys a master equation generalizing the Bloch equations for spin $\frac{1}{2}$. This equation includes terms that reflect the effects of the pumping of the different relaxation processes and also those due to the presence of external electromagnetic fields. Owing to the symmetry of the various interactions, it is usually more convenient to expand the density matrix on a set of irreducible tensors. A quite similar treatment can be applied to the photon polarization matrix by constructing its irreducible components from the standard components of the polarization vector. In this section we determine the expressions in the irreducible formalism of the terms, which have to be included in the evolution equations of the density-matrix components.

### A. Relaxation processes

*(a) Alkali-atom-buffer-gas collisions.* The perturbation suffered by an alkali-metal atom in its fundamental state when colliding with a buffer-gas molecule can be described by the action of a random magnetic field that couples with the alkali-atom electronic spin without affecting directly the nuclear part of its state. Taking into account the isotropy of the alkali-atom-gas collision process, introducing the conservation of the trace of $\rho$ and in absence of hyperfine coherences, the relaxation equations for the irreducible components of $\rho$ are [4,5]

$$[\dot{\rho}_q^K(F)]^{(c)} = -\frac{1}{T_c}\sum_{F'} {}_F^F R^K \rho_q^K(F') , \tag{1}$$

where

$$
{}^{F}_{F'}R^{K}=\tfrac{3}{4}\delta_{F,F'}+(-1)^{K+F+F'}\tfrac{3}{2}(2F+1)(2F'+1)\times\begin{Bmatrix}K & F' & F'\\ 1 & F & F\end{Bmatrix}\begin{Bmatrix}I & \frac{1}{2} & F\\ 1 & F' & \frac{1}{2}\end{Bmatrix}^{2}, \tag{2}
$$

and $T_c$ is the characteristic time constant of the relaxation by alkali-atom–gas collisions, which depend inversely on the buffer-gas pressure $P$,

$$
\frac{1}{T_c}=N_L\sigma_c\bar{v}_{\mathrm{rel}}\frac{P}{P_0}, \tag{3}
$$

where $N_L$ is Loschmidt's number, $v_{\mathrm{rel}}$ is the mean relative velocity among the colliding particles, $P_0$ is the atmospheric pressure, and $\sigma_c$ is the electronic disorientation cross section for these types of collisions. As Eq. (2) shows, the coefficients ${}^{F}_{F'}R^{K}$ are $q$ independent and, whereas the relaxation of the $k$-pole orientations of the two ground-state hyperfine levels is coupled, there is no coupling among the relaxations of the different multipole orders.

*(b) Spin-exchange collisions.* As the interaction between two colliding alkali-metal atoms is much more brief than the hyperfine period, it can be considered as being only dependent on the orientation state of the two electronic spins. However, after the collision, nuclear and electronic spins become coupled again. Following Ref. [6] and adopting the irreducible formalism in the case of two identical colliding atoms, the atomic density-matrix evolution equation under the only effect of the spin-exchange collisions has the form

$$
[\dot{\rho}^{K}_{q}(F)]^{(S)}=-\frac{1}{T_S}\left[\frac{3}{4}\rho^{K}_{q}(F)-\sum_{p}(-1)^{p}[S_p\rho S_{-p}]^{K}_{q}(F)-2\sum_{p}[S_p\rho S_{\bar{q}}-S_{\bar{q}}\rho S_p]^{K}_{q}(F)\langle S_r\rangle-\sum_{p}(-1)^{p}[S_p\rho+\rho S_p]^{K}_{q}(F)\langle S_{-p}\rangle\right], \tag{4}
$$

$S_{p,\bar{q},r}$ being the standard components of the electronic spin operator and where a cyclic permutation of the subindexes is assumed in the summations.

In Eq. (4), $T_S$ is the characteristic relaxation constant by spin-exchange collisions and depends inversely on the vapor pressure of the alkali-metal atom in the same way as in Eq. (3),

$$
\frac{1}{T_S}=N_L\sigma_S\bar{v}_{\mathrm{rel}}\frac{P}{P_0}, \tag{5}
$$

except for $\sigma_S$, which denotes the relaxation cross section by these types of collisions.

Using the expansions of the density matrix and of the spin operator standard components as a function of the standard irreducible tensorial basis, we have obtained the explicit expressions for each one of the terms included in Eq. (4):

$$
\begin{aligned}
[S_p\rho S_{\bar{q}}]^{K}_{q}(F)={}&\sum_{F'}(-1)^{2I+1}\tfrac{3}{2}(2F+1)(2F'+1)\begin{Bmatrix}\frac{1}{2} & F & I\\ F' & \frac{1}{2} & 1\end{Bmatrix}^{2}\\
&\times\sum_{\substack{K_2q_2\\K'q'}}(-1)^{K+K_2-q'-q}(2K'+1)\sqrt{(2K+1)(2K_2+1)}\\
&\times\begin{pmatrix}1 & K_2 & K'\\ p & q_2 & -q'\end{pmatrix}\begin{pmatrix}K' & 1 & K\\ q' & \bar{q} & -q\end{pmatrix}\begin{Bmatrix}1 & K_2 & K'\\ F' & F & F'\end{Bmatrix}\begin{Bmatrix}K & 1 & K\\ F & F & F'\end{Bmatrix}\rho^{K_2}_{q_2}(F'),
\end{aligned} \tag{6a}
$$

$$
\begin{aligned}
[S_p\rho+\rho S_p]^{K}_{q}(F)={}&\sum_{K_2q_2}(-1)^{F+I+\frac{3}{2}-q}\sqrt{\tfrac{3}{2}}(2F+1)\sqrt{(2K+1)(2K_2+1)}\\
&\times\begin{pmatrix}1 & K_2 & K\\ p & q_2 & -q\end{pmatrix}[(-1)^{K+K_2-1}+1]\begin{Bmatrix}\frac{1}{2} & F & I\\ F & \frac{1}{2} & 1\end{Bmatrix}\begin{Bmatrix}1 & K_2 & K\\ F & F & F\end{Bmatrix}\rho^{K_2}_{q_2}(F).
\end{aligned} \tag{6b}
$$

If $\langle S_q\rangle=0\forall q$, Eq. (4) becomes equivalent to Eq. (1), which described the relaxation by alkali-atom–gas collisions. This is so because if the alkali-metal vapor has no dipole orientation, it also presents isotropic conditions with respect to the spin-exchange collisions. However, in the presence of dipole orientation the coupled equations system (4) becomes nonlinear and the calculations are substantially complicated. On the contrary, depending on the pumping approximation adopted, only a few of the tensorial orders have to be considered in the summations.

The efficiency of the spin-exchange relaxation is very different for populations and coherences in the presence of a static magnetic field. Whereas the difference between the hyperfine levels longitudinal orientations remains constant in time, as the Landé factors corresponding to the ground-state hyperfine levels are opposite, transversal orientations are quickly destroyed by spin-exchange collisions. However, in some experiences this situation may change. For instance, if the atom is radio-frequency dressed, depending on the characteristics of the rf field, the intrinsic evolution frequencies of both levels of transversal orientations can coincide, and a resonant circulation of Zeeman coherence between the hyperfine levels becomes possible.

*(c) Alkali-atom–cell-wall collisions.* If uncoated walls are used, the collisions of the alkali-metal atoms against the cell walls after their diffusion through the buffer gas are completely disorienting. Due to this fact, the local mean value of any observable $\langle Q(\mathbf{r})\rangle$ evolves in the course of time following the diffusion equation [7]:

$$\langle \dot{Q}(\mathbf{r})\rangle = D\nabla^2\langle Q(\mathbf{r})\rangle \ , \tag{7}$$

where $D$ is the diffusion coefficient, inversely dependent on the buffer-gas pressure.

The complexity of the solution of this equation for spherical symmetry [8] advises us to approximate the totality of the relaxation modes to the dominant term (first diffusion mode approximation). In that case, and considering also the conservation of the total population, the corresponding terms of the evolution equations of the density-matrix irreducible components for $K=0$ become identical to the ones included in (1). For $K\neq 0$ the evolution equations are given by

$$[\dot{\rho}_q^K(F)]^{(d)} = -\frac{1}{T_d}\rho_q^K(F), \quad K\neq 0 \ , \tag{8}$$

where $T_d$ is the characteristic relaxation time for what concerns this process. In particular, for a spherical cell with radius $R$,

$$\frac{1}{T_d} = D\frac{\pi^2}{R^2} \ . \tag{9}$$

In practice, by using a properly dimensioned beam, the average amplitude of the second most important relaxation mode vanishes [9] and, this way, systematic errors introduced by the first diffusion mode approximation can be avoided.

In order to easily handle the expressions that describe the effects of the relaxation processes we can put together in a single term those corresponding to the alkali-atom–gas collisions, to the alkali-atom–cell-wall collisions, and the linear terms of the spin-exchange collisions, which are represented from now on by the coefficients ${}^{F}_{F'}P^K$, so that

$$[\dot{\rho}_q^K(F)]^{(c)+(d)+(sl)} = \sum_{F'} {}^{F}_{F'}P^K \rho_q^K(F') \ . \tag{10}$$

The nonlinear part of the spin-exchange collisions can be expressed as

$$[{}_F\dot{\rho}_q^K(F)]^{(snl)} = \sum_{\substack{F'K'q'\\ F''q''}} N\begin{matrix} FKq \\ F'K'q' \\ F''1q''\end{matrix}\,\rho_{q'}^{K'}(F')\rho_{q''}^{1}(F'') \ , \tag{11}$$

where the coefficients include all the nonlinear contributions from the terms in (4).

### B. Pumping process

Due to the proximity of the Larmor frequencies associated with the hyperfine levels of the ground and first excited states, the generation and circulation of Zeeman coherences during the pumping process have to be considered. Hyperfine coherences instead need not be taken into account, as the frequencies of the ground level and first excited-state hyperfine transitions are notably different. The optical excitation by the corresponding hyperfine components is considered resonant and with negligible spectral width.

#### 1. *Optical-pumping cycle*

The optical-pumping cycle may be broken up into three independent stages entirely separated in time: (a) the atom initially in the ground state is excited optically and brought to the excited state by absorbing a photon; (b) when the atom is in the excited state it has a certain probability per unit time $\Gamma_E$ of returning to the ground state by spontaneous emission; and (c) between these two processes of interaction with the optical radiation the excited state experiences its intrinsic evolution under the influence of the Zeeman effect.

In the following we are going to establish the evolution equations that describe the various stages of the optical pumping cycle for the components of the ground-state and the excited-state density matrices.

*(a) Optical excitation: Absorption process.* The action of the pumping light with polarization vector $\boldsymbol{\varepsilon}$ on the ground state is given by [10,11]

$$[\dot{\rho}(F_g)]^{(p)}_{(a)} = -\sum_{F_eF_g}[C(F_e,F_g)A_{F_e}(\boldsymbol{\varepsilon})P_{F_g}\rho_g + C^*(F_e,F_g)\rho_g P_{F_g}A^{\dagger}_{F_e}(\boldsymbol{\varepsilon})] \ , \tag{12}$$

where $P_{F_g}$ is the projector onto the multiplet $F_g$. $A_{F_e}$ is the absorption operator,

$$A_{F_e}(\boldsymbol{\varepsilon}) = \boldsymbol{\varepsilon}^*\mathbf{d}P_{F_g}\boldsymbol{\varepsilon}\mathbf{d} \ , \tag{13}$$

$\mathbf{d}$ is the transition electric dipole operator, and

$$C(F_e,F_g) = \frac{3W_p(F_e,F_g)}{2|d_{J_eJ_g}|^2} \ . \tag{14}$$

In Eq. (14) $d_{J_eJ_g}$ is the reduced matrix element of $\mathbf{d}$ between the upper and lower fine levels and the constant $W_p(F_e,F_g)$ is the so-called pumping rate of the transition $F_g\rightarrow F_e$. In the case of an isolated transition,

$$W_p(F_e,F_g) = \frac{8\pi^2}{3hc}|d_{J_eJ_g}|^2 d\Omega\, I_p(F_e,F_g) \ , \tag{15}$$

where $I_p(F_e,F_g)$ is the spectral intensity of the radiation at the central frequency of the transition and $d\Omega$ is the solid angle subtended by the pumping beam.

The expression for the operator $A_{F_e}$, as a function of the standard irreducible operators constructed from the angular momenta $F_g$ and $F'_g$, is

$$A_{F_e}(\varepsilon)=\sum_{F_g F'_g K q}\phi_q^K(\varepsilon^*)B_K(F_g,F'_g,F_e)T_q^K(F_g,F'_g)\ . \tag{16}$$

In expression (16), $\phi_q^K$ are the components of a second-degree tensor constructed from the components of the polarization vector $\varepsilon$ [12], whereas the coefficients

$$B_K(F_g,F'_g,F_e)=(-1)^{F_g+F_e+K+1}\begin{Bmatrix} F_g & F'_g & K \\ 1 & 1 & F_e \end{Bmatrix} \times d_{F_eF_g}d^*_{F_eF_g} \tag{17}$$

yield the dependence upon the line strengths and upon the angular momenta involved.

The operator $A_{F_e}$ appears in Eq. (12) within a product with the density matrix $\rho$, and accordingly a new decomposition of this product into irreducible components is required. There results a mixing of the different $k$ components of the ground-state density matrix, except in the case of weak atomic polarization or weak pumping light, where $\rho_g$ can be considered as proportional to $P_g$ in the first approximation. Including, as was mentioned before, the possibility of the generation of Zeeman coherences, but not of the hyperfine ones, the evolution of irreducible components of the ground-state density matrix caused by the absorption process is given by

$$[\dot{\rho}_{q_g}^{K_g}(F_g)]_{(a)}^{(p)}=-\sum_{F_e}W_p(F_g,F_e)\sum_{K'_g q'_g}B_{1\,K'_g q'_g}^{\;K_g q_g}(F_e,F_g,\varepsilon)\rho_{q'_g}^{K'_g}(F_g)\ , \tag{18}$$

where in order to simplify subsequent expressions we have introduced a set of coefficients $B_{1\,B'_g q'_g}^{\;K_g q_g}(F_e,F_g,\varepsilon)$ defined by

$$\begin{aligned} B_{1\,K'_g q'_g}^{\;K_g q_g}(F_e,F_g,\varepsilon)={}&(-1)^{F_g+F_e+q_g+1}\tfrac{3}{2}(2F_e+1)(2F_g+1)\begin{Bmatrix} J_e & 1 & J_g \\ F_g & I & F_e \end{Bmatrix}^2 \\ &\times\sqrt{(2K_g+1)(2K'_g+1)}\left[\sum_{K_1 q_1}(-1)^{K_1}\phi_{q_I}^{K_1}(\varepsilon)\begin{Bmatrix} F_g & F_g & K_1 \\ 1 & 1 & F_e \end{Bmatrix}\sqrt{2K_1+1}\right. \\ &\left.\times\begin{Bmatrix} K_1 & K'_g & K_g \\ F_g & F_g & F_g \end{Bmatrix}\begin{pmatrix} K_1 & K'_g & K_g \\ q_1 & q'_g & -q_g \end{pmatrix}[(-1)^{K_g+K'_g}+(-1)^{K_1}]\right]\ . \end{aligned} \tag{19}$$

The pumping beam polarization $\varepsilon$ through the tensor $\phi_q^K(\varepsilon)$ together with $3J$ and $6J$ coefficients selection rules determine which of the $B_{1\,K'_g q'_g}^{\;K_g q_g}(F_e,F_g,\varepsilon)$ are different from zero, and which tensorial components can be generated in the ground state by depopulation. Logically, no coupling appears among tensorial components of different hyperfine levels.

The evolution equation of the excited-state density matrix, which describes the effect of the absorption process, is

$$[\dot{\rho}(F_e)]_{(a)}^{(p)}=C(F_e,F_g)\varepsilon\,\mathbf{d}\rho_g\varepsilon^*\mathbf{d}\ , \tag{20}$$

and in the same way as in (12), for the sake of generality, the density matrix $\rho_g$ may be polarized. Evaluating the factors in (20), and introducing the set of coefficients $B_{e\,F_g K_g q_g}^{\;F_e K_e q_e}(\varepsilon)$, defined as

$$\begin{aligned} B_{e\,F_g K_g q_g}^{\;F_e K_e q_e}(\varepsilon)={}&(-1)^{K_g+q_e}3(2F_e+1)(2F_g+1)\sqrt{(2K_e+1)(2K_g+1)}\begin{Bmatrix} J_e & 1 & J_g \\ F_g & 1 & F_e \end{Bmatrix}^2 \\ &\times\sum_{K_1 q_1}(-1)^{K_1}\phi_{q_1}^{K_1}(\varepsilon)\sqrt{2K_1+1}(-1)^{K_1}\begin{pmatrix} K_g & K_1 & K_e \\ q_g & q_1 & -q_e \end{pmatrix}\begin{Bmatrix} F_e & F_g & 1 \\ F_e & F_g & 1 \\ K_e & K_g & K_1 \end{Bmatrix}\ , \end{aligned} \tag{21}$$

expression (20) gives

$$[\dot{\rho}_{q_e}^{K_e}(F_e)]_{(a)}^{(p)}=-\sum_{F_g}W_p(F_g,F_e)\sum_{K_g q_g}B_{e\,F_g K_g q_g}^{\;F_e K_e q_e}(\varepsilon)\rho_{q_g}^{K_g}(F_g)\ . \tag{22}$$

The coefficients $B_{e\,F_g K_g q_g}^{\;F_e K_e q_e}(\varepsilon)$ comprise all the geometrical dependence and also the dependence upon the line strengths of the absorption process. The tensor $\phi_q^K(\varepsilon)$ included in (21) yields again the dependence upon the pumping beam polarization and determines which excited-state tensorial components can be generated by the optical excitation.

*(b) Spontaneous emission process.* The evolution of the excited-state density matrix is described by

$$[\dot{\rho}_{q_e}^{K_e}(F_e)]_{(b)}^{(p)}=-\Gamma_E\rho_{q_e}^{K_e}(F_e)\ , \tag{23}$$

where

$$\Gamma_E=\frac{4k^3}{3(2J_e+1)\hbar}|d_{J_eJ_g}|^2 \tag{24}$$

is the inverse of the mean lifetime of the excited level and $2\pi/k$ is the transition wavelength.

On the other hand, the evolution of the ground-state density matrix can be expressed in the form

$$[\dot{\rho}^{K_g}_{q_g}(F_g)]^{(p)}_{(b)}=\sum_{F_e} A(F_e,F_g)(-1)^{F_e+F_g+K_g+1}(2F_e+1)\begin{Bmatrix} F_e & F_e & K_g \\ F_g & F_g & 1 \end{Bmatrix}\rho^{K_g}_{q_g}(F_e) , \tag{25}$$

where $A(F_e,F_g)$ is the Einstein coefficient of the hyperfine transition.

Equation (25) can also be expressed as a function of the same parameter $\Gamma_E$ by using the relation

$$d_{F_eF_g}=(-1)^{J_e+F_g+I+1}\sqrt{(2F_e+1)(2F_g+1)}\times\begin{Bmatrix} J_e & 1 & J_g \\ F_g & I & F_e \end{Bmatrix}d_{J_eJ_g} \tag{26}$$

yielding

$$[\dot{\rho}^{K_g}_{q_g}(F_g)]^{(p)}_{(b)}=\Gamma_E\sum_{F_e}B_2(F_g,F_e,K_g)\rho^{K_g}_{q_g}(F_e) . \tag{27}$$

We have introduced another set of coefficients $B_2(F_g,F_e,K_g)$ defined as

$$B_2(F_g,F_e,K_g)=2(2F_g+1)\begin{Bmatrix} J_e & 1 & J_g \\ F_g & I & F_e \end{Bmatrix}^2(-1)^{F_e+F_g+K_g+1}\times(2F_e+1)\begin{Bmatrix} F_e & F_e & K_g \\ F_g & F_g & 1 \end{Bmatrix} . \tag{28}$$

Whereas in the absorption process the pumping beam with given propagation and polarization vectors introduces privileged directions, and accordingly diverse sublevels absorb light in a different way, the emission process is isotropic, having all the sublevels the same mean lifetime and giving rise to the $q$ independence of the coefficients $B_2$. As there is no coupling in (27) between different tensorial orders, only those tensorial components already present in the excited state may be generated in the ground state by spontaneous emission.

*(c) Intrinsic evolution under the influence of the external magnetic field.* The excited-state density-matrix components evolve in the form

$$[\dot{\rho}^{K_e}_{q_e}(F_e)]^{(p)}_{(c)}=-iq_e\omega_{F_e}\rho^{K_e}_{q_e}(F_e) , \tag{29}$$

where $\omega_{F_e}$ is the Larmor frequency of the excited level $F_e$. Although it has no direct influence on the coefficients that characterize the pumping process, an analogous term of intrinsic evolution of the ground-state density-matrix tensorial components will have to be considered when completing the total evolution equations system.

### 2. Pumping matrix

By adding the effects of the three stages of the pumping process and taking into account that for heavy alkali-metal atoms and under ordinary working conditions the relaxation in the excited level can be considered as only caused by the alkali-atom–gas collisions [13], the overall evolution equation for the components of the excited-state density matrix has the form

$$[\dot{\rho}^{K_e}_{q_e}(F_e)]^{(p)+(c)}=\sum_{F_gK_gq_g}W_p(F_g,F_e){B_e}^{F_eK_eq_e}_{F_gK_gq_g}(\boldsymbol{\varepsilon})\rho^{K_g}_{q_g}(F_g)-\Gamma_E\rho^{K_e}_{q_e}(F_e)-\sum_{F_e'}{}^{F_e}_{F_e'}P^{K_e}\rho^{K_e}_{q_e}(F_e')-iq_e\omega_{F_e}\rho^{K_e}_{q_e}(F_e) . \tag{30}$$

By using this expression, the dependence of the evolution of the ground-state components on the excited-state components that reflects (27) can be eliminated. We differentiate two cases.

*(a) Evolution of the ground-state populations.* Due to the spontaneous emission characteristics, only the excited-state population can contribute to the evolution of the ground-state populations. However, the excited-state populations may have been generated from the ground-state coherences and therefore the evolution of ground-state populations and coherences becomes coupled.

As it was pointed out in case (a) of Sec. II A the relaxation by alkali-atom–buffer-gas collisions of same-order population belonging to the excited-state different hyperfine levels is coupled. The equations included in the equation system (38) can then be uncoupled by diagonalizing the relaxation $(2J_e+1)$-dimension matrix constituted by the corresponding coefficients defined in Eq. (2). If the change of basis associated with the diagonalization process is done, the now uncoupled evolution equations of the relaxation eigenobservables by alkali-atom–gas collisions $\langle V^{K_e}_i\rangle$ [1] can be written as

$$\langle\dot{V}^{K_e}_i\rangle=\sum_{F_e}C_{K_e}(i,F_e)\sum_{F_gK_gq_g}W_p(F_g,F_e){B_e}^{F_eK_e0}_{F_gK_gq_g}(\boldsymbol{\varepsilon})\rho^{K_g}_{q_g}(F_g)-\Gamma_E\langle V^{K_e}_i\rangle-\Gamma^{K_e}_i\langle V^{K_e}_i\rangle , \tag{31}$$

where

$$\langle V_i^{K_e} \rangle = \sum_{F_e} C_{K_e}(i,F_e) \langle T_0^{K_e}(F_e) \rangle \ , \tag{32}$$

and $\Gamma_i^{K_e}$ are the relaxation-time constants of the eigenobservables.

Taking (31) into account, we can determine the stationary mean values of these eigenobservables,

$$\langle V_i^{K_e} \rangle = \frac{\sum_{F_e} C_{K_e}(i,F_e) \sum_{F_g K_g q_g} W_p(F_g,F_e) B_{e\,F_g K_g q_g}^{\;F_e K_e 0}(\varepsilon) \rho_{q_g}^{K_g}(F_g)}{\Gamma_E + \Gamma_i^{K_e}} \ . \tag{33}$$

In order to undo the change of basis we have to use the adjoint matrix of the one in (32). This way, we can obtain the expression for the stationary values of the excited-state populations, and if they are substituted in (27), the evolution of the ground-state populations caused by the spontaneous emission becomes

$$\begin{aligned}[\dot{\rho}_0^{K_g}(F_g)]^{(p)} = & -\sum_{F_e} W_p(F_g,F_e) \sum_{K_g'} B_{1\,K_g' 0}^{\;K_g 0}(F_e,F_g,\varepsilon) \rho_0^{K_g'}(F_g) + \Gamma_E \sum_{F_E} B_2(F_g,F_e,K_g) \\ & \times \sum_i C_{K_g}(i,F_e) \frac{\sum_{F_e} C_{K_g}(i,Fe') \sum_{F_g' K_g' q_g'} W_p(F_g',F_e') B_{e\,F_g' K_g' q_g'}^{\;F_e' K_g 0}(\varepsilon) \rho_{q_g'}^{K_g'}(F_g')}{\Gamma_E + \Gamma_i^{K_g}} \ , \end{aligned} \tag{34}$$

where any dependence upon excited-state components has been eliminated

*(b) Evolution of the ground-state Zeeman coherences.* We assume the secular approximation, that is, the coupling is only possible between those components that evolve under the effect of the external magnetic field at the same frequencies.

Due to the excited-state intrinsic evolution term it is more advisable to adopt the interaction representation with respect to the Hamiltonian that includes the effect of the static magnetic field $H_0$, so that

$$[\dot{\rho}_{q_e}^{K_e}(F_e)]^{(p)+(c)} = \sum_{F_g K_g q_g} W_p(F_g,F_e) B_{e\,F_g K_g q_g}^{\;F_e K_e q_e}(\varepsilon) \rho_{q_g}^{K_g}(F_g) e^{i[q_e \omega_{F_e} - q_g \omega_{F_g}]t} - \Gamma_E \rho_{q_e}^{K_e}(F_e) - \sum_{F_e'} {}_{F_e'}^{F_e}P^{K_e} \rho_{q_e}^{K_e}(F_e') e^{i[q_e \omega_{F_e} - q_g \omega_{F_e'}]t} \ . \tag{35}$$

Each excited-state tensorial component is only coupled by collisions to itself so that no diagonalization is necessary, and we directly obtain

$$[\rho_{q_e}^{K_e}(F_e)]^{(p)+(c)} = \sum_{F_g K_g q_g} \frac{W_p(F_g,F_e) B_{e\,F_g K_g q_g}^{\;F_e K_e q_e}(\varepsilon) \rho_{q_g}^{K_g}(F_g) e^{i[q_e \omega_{F_e} - q_g \omega_{F_g}]t}}{\Gamma_E + {}_{F_e}^{F_e}P^{K_e} + i[q_e \omega_{F_e} - q_g \omega_{F_g}]} \ . \tag{36}$$

If (36) is substituted in expression (27) once it has been transformed into the interaction representation,

$$[\dot{\rho}_{q_g}^{K_g}(F_g)]_{(b)}^{(p)} = \Gamma_E \sum_{F_e} B_2(F_g,F_e,K_g) \rho_{q_g}^{K_g}(F_e) e^{i[q_g(\omega_{F_g} - \omega_{F_e})]t} \ , \tag{37}$$

we can write

$$[\dot{\rho}_{q_g}^{K_g}(F_g)]_{(b)}^{(p)} = \Gamma_E \sum_{F_e} B_2(F_g,F_e,K_g) \sum_{F_g' K_g' q_g'} \frac{W_p(F_g',F_e) B_{e\,F_g' K_g' q_g'}^{\;F_e K_g q_g}(\varepsilon) \rho_{q_g'}^{K_g'}(F_g') e^{i[q_g(\omega_{F_g} - \omega_{F_e}) + (q_g \omega_{F_e} - q_g' \omega_{F_g'}]t}}{\Gamma_E + {}_{F_e}^{F_e}P^{K_g} + i[q_g \omega_{F_e} - q_g' \omega_{F_g'}]} \ . \tag{38}$$

Adopting again the secular approximation, the summation in the second member is restricted only to those values of $q_g'$ that verify $q_g \omega_{F_g} = q_g' \omega_{F_g'}$. We finally obtain

$$[\dot{\rho}_{q_g}^{K_g}(F_g)]^{(p)} = -\sum_{F_e} W_p(F_g,F_e) \sum_{K_g' q_g'} B_{1\,K_g' q_g'}^{\;K_g q_g}(F_e,F_g,\varepsilon) \rho_{q_g'}^{K_g'}(F_g) + \Gamma_E \sum_{F_e} B_2(F_g,F_e,K_g) \sum_{F_g' K_g'} \frac{W_p(F_g',F_e) B_{e\,F_g' K_g' q_g'}^{\;F_e K_q q_g}(\varepsilon) \rho_{q_g'}^{K_g'}(F_g')}{\Gamma_E + {}_{F_e}^{F_e}P^{K_g} + i[q_g(\omega_{F_e} - \omega_{F_g})]} \ . \tag{39}$$

In order to describe in a compact way the effects of the pumping process on the ground-state tensorial components we define a pumping matrix which comprises both Eq. (34) and Eq. (39), so that we write

$$[\dot{\rho}_q^K(F)]^{(p)} = \sum_{F'K'q'} \lambda_{F'K'q'}^{FKq} \rho_{q'}^{K'}(F') \ . \tag{40}$$

The characteristics of pumping processes can be deduced by observing which of the elements of the pumping matrix are different from zero and therefore which of the tensorial components may be generated.

## III. STATIONARY STATE

In order to obtain the stationary values of the ground-state density-matrix tensorial components, the homogeneous system associated to the one formed by their evolution equations has to be solved. If we group together the terms analyzed in section II we can write the complete evolution equations as

$$[\dot{\rho}_q^K(F)] = \sum_{F'} {}_{F'}^{F}P^K \rho_q^K(F') + \sum_{\substack{F'K'q' \\ F''q''}} N_{F'K'q'\ F''1q''}^{FKq} \rho_{q'}^{K'}(F') \rho_{q''}^{1}(F'') + \sum_{F'K'q'} \lambda_{F'K'q'}^{FKq} \rho_{q'}^{K'}(F') - iq\omega_F \rho_q^K(F) \ . \tag{41}$$

This system has to be completed with a normalization condition. If the intensity of the detection beam is considered as negligible, and hence it does not affect significantly the stationary atom distribution, it seems reasonable to adopt as a normalization condition that which guarantees the conservation of the total population inside the ground level and the excited levels involved in the pumping process:

$$\sum_{F_g} \sqrt{2F_g+1}\,\rho_0^0(F_g) + \sum_{F_e} \sqrt{2F_e+1}\,\rho_0^0(F_e) = 1 \ . \tag{42}$$

By using the same procedure as with the pumping process, the terms depending on the excited-state components can be eliminated from the normalization equation, yielding

$$\sum_{F_g} \sqrt{2F_g+1}\,\rho_0^0(F_g) + \sum_{F_e} \sqrt{2F_e+1} \sum_i C_0(F_e,i) \frac{\sum_{F_e'} C_0(i,F_e') \sum_{F_g'} W_p(F_g',F_e') \sum_{K_g'} B_{e\,F_e'00}^{\,F_g'K_g'q_g'}(\varepsilon) \rho_{q_g'}^{K_g'}(F_e)}{\Gamma_E + \Gamma_i^0} = 1 \ . \tag{43}$$

The polarization of the pumping beam, through the coefficients $B_{e\,F_e'00}^{\,F_g'K_g'q_g'}(\varepsilon)$, included in (43), determines which ground-state tensorial components have a nonzero contribution to the evolution of the $\rho_0^0(F_e)$ and therefore are present in the normalization equation.

## IV. LIGHT ABSORPTION BY OPTICALLY PUMPED ALKALI-METAL VAPORS

The variation that a light beam experiences when it passes through an optically pumped alkali-metal vapor is determined by the change in the number of atoms in the ground state. This change is related to the instantaneous values of the density-matrix components. Therefore, the orientation state of the atom assembly can be studied by analyzing the modifications produced on a resonant crossing light beam.

The dependence of that variation can be expressed as

$$\Delta I \propto \sum_{F_g} \sqrt{2F_g+1}\,\rho_0^0(F_g) \ , \tag{44}$$

and from (12),

$$\Delta I \propto \mathrm{Tr} \left| -\sum_{F_eF_g} [C(F_e,F_g) A_{F_e}(\varepsilon) P_{F_g} \rho_g + \text{c.c.}] \right| \ . \tag{45}$$

Taking this and expansion (16) into account, we obtain

$$\Delta I \propto \sum_{F_gF_e} W_d(F_g,F_e) \sum_{K_q} B_{Dq}^{K}(F_g,F_e,\varepsilon) \rho_q^K(F_g) \ , \tag{46}$$

where $W_d(F_g,F_e)$ are the intensities of the hyperfine components and the coefficients $B_{Dq}^{K}(F_g,F_e,\varepsilon)$ are geometrical factors and, as could be expected, coincide with the coefficients $B_1$ defined in (19) for $K=q=0$:

$$B_{Dq}^{K}(F_g,F_e,\varepsilon) = B_{1Kq}^{00}(F_g,F_e,\varepsilon) \ . \tag{47}$$

If we substitute the stationary values of the density-matrix components in Eq. (46) we can separate the contributions of each multipole order to the variations that the detection beam experiences and therefore deduce the suitable orientation, polarization, and spectral distribution of that detection beam in order to measure any tensorial component, either populations or coherences.

## V. NUMERICAL RESULTS

In order to show the applicability of the expressions obtained in the previous sections, we are going to analyze the dependences of the stationary values of the density-matrix components by solving numerically their evolutions (41) for a particular system. The alkali-metal atom that we have selected is cesium, as it has been the one mostly used in our laboratory. For our calculations we assume the intermediate pumping approximation, that is, we consider that the only multipole orientations that can be generated by the pumping process are the hyperfine, dipole, and quadrupole. In practice, this means that we only have to include in our equations tensorial components with $K \leq 2$.

### A. Coefficients involved in the evolution equations for cesium

Before calculating the stationary values of the density-matrix components, several sets of coefficients that appear in the terms of the evolution equations have to be computed for the particular case of cesium. The coefficients ${}^{F}_{F'}R^{K}$, which are present in the alkali-atom–gas-collision term are defined in Eq. (2). Their values for the Cs ground state are given in Table I. From these values, the relaxation-time constants of the eigenobservables by alkali-atom–gas collisions $V_i^K$ are

$$\Gamma_{+}^{K}=\frac{1}{T_c}\frac{K(K+1)}{64}\,,\quad \Gamma_{-}^{K}=\frac{1}{T_c}\,, \tag{48}$$

$T_c$ being the one in (3).

As was noted in case (b) of Sec II A when there is no dipole orientation the relaxation coefficients by spin-exchange collisions reduce to the ones by alkali-atom–gas collisions (Table I). Nevertheless, their evaluation in the presence of dipole orientation using (6a) and (6b) becomes more difficult and in this case the large number of nonzero coefficients would require an extensive tabulation. The values obtained from our completely general expressions coincide for cesium and, in the absence of coherences, with the particular ones tabulated for the relaxation by spin exchange of the $\langle V_i^K\rangle$ in Ref. [2].

The values of the pumping matrix elements depend on the polarization and spectral distribution of the pumping light, so that they have to be calculated for each case and cannot be tabulated. It is so with the sets of pumping coefficients $B_{1\,K_g'q_g'}^{\;K_gq_g}(F_e,F_g,\varepsilon)$ and $B_{e\,F_gK_gq_g}^{\;F_eK_eq_e}(\varepsilon)$, which where introduced in Eqs. (19) and (21) as they also depend on the pumping beam polarization. Spontaneous emission coefficients $B_2(F_g,F_e,K_g)$ for cesium, instead, are given in Table II. The only previous results with which we can compare, in this case, the values that we obtain for all these sets of coefficients from our general expressions are the ones in Ref. [2] that correspond to cesium $\sigma^{\pm}$polarization pumping. In this particular case we obtain equal values. In order to compute the pumping matrix we also need to determine, as Eq. (38) shows, the relaxation coefficients by alkali-atom–gas collisions for the cesium excited states, which are involved in the pumping process. If, for simplicity, we consider $D_1$ pumping, the corresponding coefficients are also the same as the ones in Table I. Lastly, as we pointed out in Sec. IV, the coefficients $B_{D\,q}^{\;K}(F_g,F_e,\varepsilon)$ that take part in the detection process coincided with the pumping $B_{1\,K_g'q_g'}^{\;K_gq_g}(F_e,F_g,\varepsilon)$ coefficients when $K=q=0$, and therefore depend also on the pumping beam polarization.

TABLE I. Relaxation coefficients by alkali-atom–buffer-gas collisions ${}^{F}_{F'}R^{K}$ for the density-matrix components of the cesium ground state.

| $K$ | $F$ | $F'$ | ${}^{F}_{F'}R^{K}$ |
|---|---|---|---|
| 0 | 3 | 3 | $\frac{9}{16}$ |
| 0 | 3 | 4 | $-3\sqrt{7}/16$ |
| 0 | 4 | 3 | $-3\sqrt{7}/16$ |
| 0 | 4 | 4 | $\frac{7}{16}$ |
| 1 | 3 | 3 | $\frac{37}{64}$ |
| 1 | 3 | 4 | $-3\sqrt{105}/64$ |
| 1 | 4 | 3 | $-3\sqrt{105}/64$ |
| 1 | 4 | 4 | $\frac{29}{64}$ |
| 2 | 3 | 3 | $\frac{39}{64}$ |
| 2 | 3 | 4 | $-5\sqrt{33}/64$ |
| 2 | 4 | 3 | $-5\sqrt{33}/64$ |
| 2 | 4 | 4 | $\frac{31}{64}$ |

TABLE II. Spontaneous emission coefficients $B_2(F_g,F_e,K_g)$ between the hyperfine levels of the cesium ground and first excited states.

| $F_g$ | $F_e$ | $K$ | $B_2$ |
|---|---|---|---|
| 3 | 3 | 0 | $\frac{1}{4}$ |
| 3 | 4 | 0 | $\sqrt{7}/4$ |
| 3 | 3 | 1 | $\frac{11}{48}$ |
| 3 | 4 | 1 | $\sqrt{105}/16$ |
| 3 | 3 | 2 | $\frac{3}{16}$ |
| 3 | 4 | 2 | $5\sqrt{33}/48$ |
| 4 | 3 | 0 | $\sqrt{7}/4$ |
| 4 | 4 | 0 | $\frac{5}{12}$ |
| 4 | 3 | 1 | $\sqrt{105}/16$ |
| 4 | 4 | 1 | $\frac{19}{48}$ |
| 4 | 3 | 2 | $5\sqrt{33}/48$ |
| 4 | 4 | 2 | $\frac{17}{48}$ |

### B. Stationary values of the density-matrix components

Our calculations have been realized for the system Cs+20-Torr Ar. For the values of the characteristic constants of the relaxation processes for the ground state, we have assumed those given in Ref. [3]: $\sigma_c=104\times10^{-23}\,\mathrm{cm}^2$; $\sigma_S=1.63\times10^{-14}\,\mathrm{cm}^2$; $D_0=0.101\,\mathrm{cm}^2\,\mathrm{s}^{-1}$. The cesium vapor is contained in a spherical cell ($R=2.5$ cm) at $T=300$ K. The density of cesium atoms, $\rho_{\mathrm{Cs}}=5.54\times10^{10}\,\mathrm{at\,cm}^{-3}$, has been evaluated by using the Langmuir-Taylor formula [14]. In these conditions the relaxation times by the relaxation processes are, respectively, $1/T_d=6.98$, $1/T_c=30.44$, $1/T_s=27.91$. In what concerns the excited level, we adopt for its relaxation cross section by Cs-Ar collisions the value $\sigma_e=5.6\times10^{-16}\,\mathrm{cm}^2$ [15] and for the mean lifetime of the level $\Gamma^{-1}=3.4\times10^{-8}$ s [16], so that $1/T_e=1.64\times10^{7}$.

We are going to analyze first the generation of longitudinal components (i.e., the populations of the levels), and secondly we will consider that of the transversal components (i.e., the Zeeman coherences).

*(a) Longitudinal components.* In order to show the stationary-state situation, the equilibrium values of the relaxation eigenobservables by alkali-atom–gas collisions are usually used as they can be readily expressed in terms of the angular observables [2]. In Fig. 1 the equilibrium

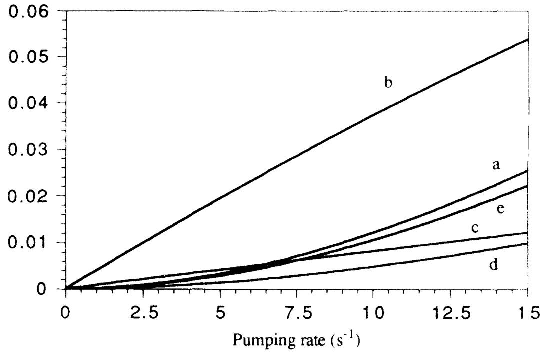

FIG. 1. Equilibrium mean values of the relaxation eigenobservables by alkali-atom–gas collisions $\langle V_i^K\rangle$ induced by pumping with $\sigma^+$-polarized white light vs pumping rate $W_p$: (a) $\langle V_-^0\rangle\times 10$, (b) $\langle V_+^1\rangle$, (c) $\langle V_-^1\rangle$, (d) $\langle V_+^2\rangle$, (e) $\langle V_-^2\rangle\times 10$.

values of $\langle V_i^K\rangle$, $i=+,-$, for pumping with $\sigma^+$-polarized white light, are represented as a function of the pumping rate. It can be seen how in this case of uniform spectrum, the dipole orientation, which has been directly generated, depends on the pumping rate in an approximately linear form, whereas even-$K$ orientations, which have been generated in second order, present a square-law dependence.

Unlike for rubidium through isotropic pumping, for cesium there is no possibility of efficient hyperfine pumping with classic spectral sources of light. However, if the intensities of the two hyperfine lines $i_+$ and $i_-$ are unbalanced or if the intensities of the two components of each of those lines are also unbalanced, a detectable hyperfine orientation accompanied by alignment can be achieved. As an example of this, in Fig. 2, the relative differences in the equilibrium values $\langle V_i^K\rangle$, when compared to those plotted in Fig. 1, are represented versus the difference of pumping rate between the two lines $i_+$ and $i_-$ for pumping with $\sigma^+$-polarized light and $W_p=5$. Hyperfine pumping presents the strongest dependence on the difference between pumping rates as it turns to be generated in first order, whereas dipole orientation shows relatively little dependence. We have supposed the same intensity for the two hyperfine components of each of the lines; otherwise there is also a direct generation of quadrupole orientation.

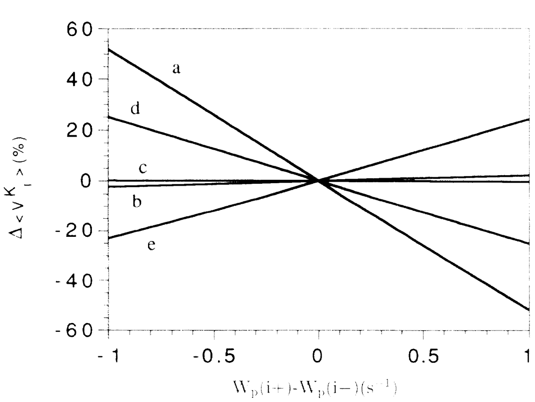

FIG. 2. Relative differences in the equilibrium values of $\langle V_i^K\rangle$ represented in Fig. 1 for $W_p=5$ vs the difference of pumping rate between the hyperfine lines $[W_p(i+)-W_p(i-)]$: (a) $\langle V_-^0\rangle/5$, (b) $\langle V_+^1\rangle$, (c) $\langle V_-^1\rangle$, (d) $\langle V_+^2\rangle$, (e) $\langle V_-^2\rangle$.

*(b) Transversal components.* Transversal pumping can induce Zeeman coherences. Their stationary-state values are nonnegligible and present a resonant behavior near zero magnetic field, the known Hanle effect. In Figs. 3(a) and 3(b) we represent, respectively, the values of the real and imaginary parts of the transversal components of the density matrix, ${}_F\rho_q^K$, induced by pumping with uniform spectrum, transversal $\sigma^+$-polarized light, and $W_p=3$, as a function of the ground-state Larmor frequency. The population of the levels, due to their coupling with the Zeeman coherences, also exhibit the so-called "zero-field saturation resonance." We represent in Fig. 4 the dependences of the mean values $\langle V_i^K\rangle, i=+,-$ on the ground-state Larmor frequency for the same pumping parameters. Due to the pumping beam characteristics the hyperfine and quadrupole orientation represented in Fig. 4 can only be generated through their coupling with the coherences. That is why their values approach zero far from the zero magnetic field.

In Fig. 5 the amplitudes of the resonances of the Zeeman coherences represented in Figs. 3(a) and 3(b) are plotted as a function of the pumping rate. It can be ob-

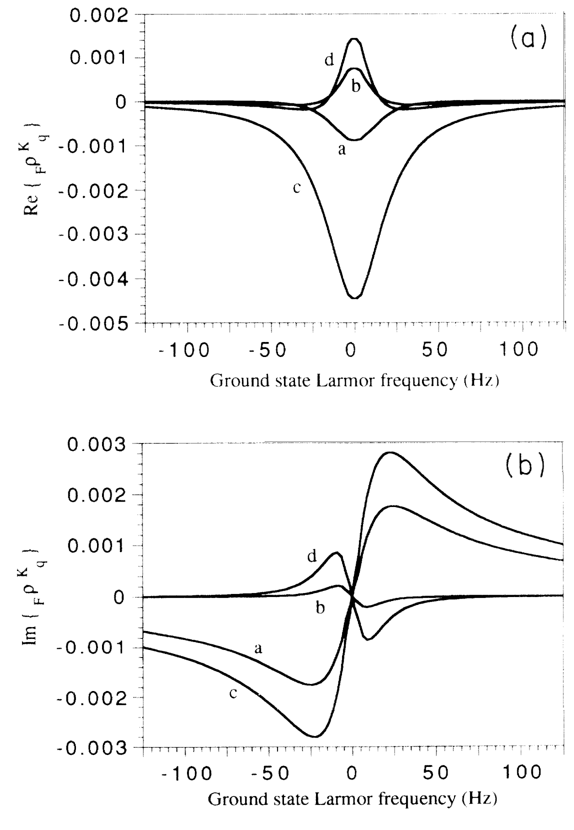

FIG. 3. (a) and (b) Real and imaginary parts, respectively, of the transversal components of the atomic density matrix induced by pumping with transversal $\sigma^+$-polarized white light as a function of the ground-state Larmor frequency [(a) lower level, (b) upper level]: (a) ${}_a\rho_1^1$, (b) ${}_a\rho_2^2\times 10$, (c) ${}_b\rho_1^1$, (d) ${}_b\rho_2^2\times 10$.

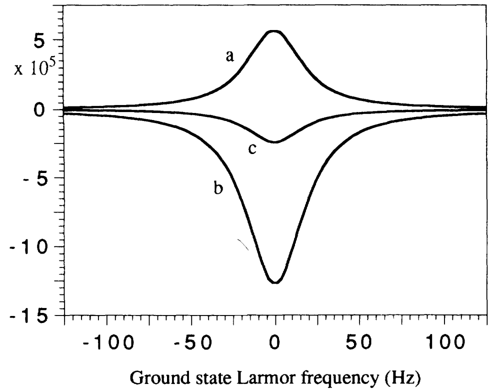

FIG. 4. "Zero-field saturation resonances" experienced by the equilibrium mean values of the relaxation eigenobservables by alkali-atom–gas collisions $\langle V_i^K \rangle$ induced by pumping with transversal $\sigma^+$-polarized white light vs the ground-state Larmor frequency: (a) $\langle V_-^0 \rangle$, (b) $\langle V_+^2 \rangle$, (c) $\langle V_-^2 \rangle$.

served clearly how for these pumping beam characteristics the lower level dipole coherence, directly generated, tends to decrease for higher pumping rates, as the other coherences that are generated from it in second order increase.

We have analyzed the influence of the nonlinear term in Eq. (41) by calculating the stationary mean values without considering that term and using them as starting values for a Newton-Rhaphson method. The nonlinear term introduces no qualitative changes and after three or four iterations the stationary mean values converge up to $10^{-6}$.

### C. Detection process

As it could be expected, the detection signals present a strong dependence on the multipole character and on the spectral uniformity of both the pumping and the detection beam. These dependences can be revealed by using Eq. (46) to compute the changes experienced by the detection beam intensity.

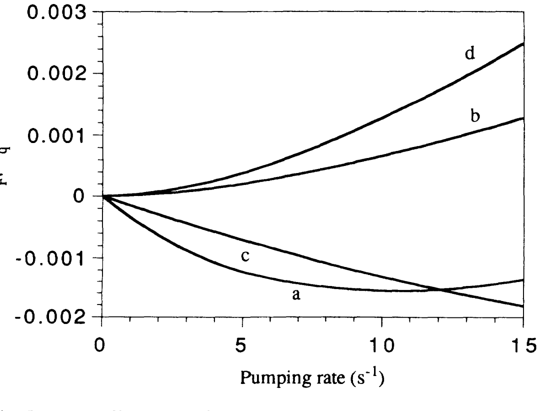

FIG. 5. Amplitudes of the Zeeman-coherences resonances represented in Figs. 3(a) and 3(b) as a function of the pumping rate: (a) $\langle {}_a\rho_1^1 \rangle$, (b) $\langle {}_a\rho_2^2 \rangle$, (c) $\langle {}_b\rho_1^1 \rangle$, (d) $\langle {}_b\rho_2^2 \rangle$.

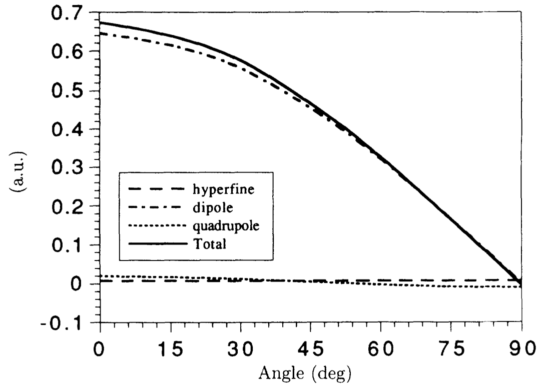

FIG. 6. Detection signal and different multipole contributions to this signal as a function of the angle $\theta$ between the propagation direction of the $\sigma^+$-polarized detection beam and the $z$ axis defined by the static magnetic field. The pumping beam is $\sigma^+$ polarized with a strongly unbalanced spectrum: $W_p(F_g=3 \rightarrow F_e=3) = W_p(F_g=4 \rightarrow F_e=3) = 4$; $W_p(F_g=3 \rightarrow F_e=4) = W_p(F_g=4 \rightarrow F_e=4) = 6$.

The multipole character of the detection beam can be modified for instance by rotating its propagation direction. In Fig. 6 we represent the detection signal together with the different multipole contributions to this signal versus $\theta$, the angle between the propagation direction of the $\sigma^+$-polarized detection beam and the $z$ axis defined by the static magnetic field. The pumping beam is $\sigma^+$-polarized and it has an unbalanced spectrum. We can observe that the largest contribution to the detection profile is by far that of the dipole orientation, but there are nonnegligible contributions of both the hyperfine and the quadrupole orientations. Whereas the hyperfine contribution remains constant, the quadrupole goes from positive to negative values, being zero for $\cos\theta = 1/\sqrt{3}$.

In Fig. 7 the dependence of the detection signal on the spectrum uniformity of the pumping beam can be seen in a case of presence of Zeeman coherences. Due to the detection beam characteristics only the hyperfine orientation and the quadrupole coherences, but not the dipole or

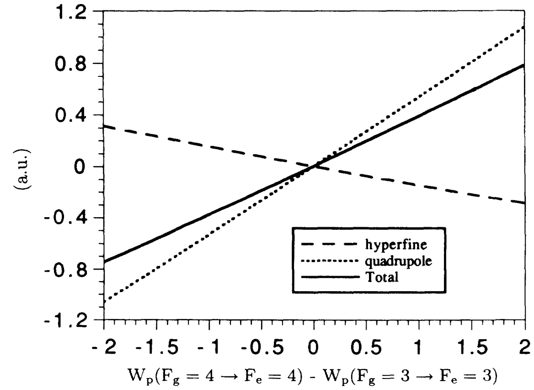

FIG. 7. Dependence of the detection signal on the spectral uniformity of the pumping beam. The pumping beam is $\sigma$ polarized and the intensities of the components of the hyperfine lines are as in Fig. 6. We represent the detection signal and the contributions to this signal as a function of the difference between $W_p(F_g=3 \rightarrow F_e=4) = W_p(F_g=4 \rightarrow F_e=4)$ and $W_p(F_g=3 \rightarrow F_e=3) = W_p(F_g=4 \rightarrow F_e=3)$.

quadrupole orientation, can contribute to the detection profile. We can see how these contributions change strongly for unbalanced pumping beam spectra.

The dependence on the detection beam characteristics of the detection profiles in situation of resonance of the Zeeman coherences can also be analyzed. Figures 8(a) and 8(b) show the detection profiles and the contributions to these profiles from the populations and Zeeman coherences, for two cases with the same $\sigma^+$-polarized pumping beam and where only the detection beam differs. It can be seen how the signal shape may change completely. In Fig. 8(a) the two-maxima signal results from the addition of the one-maximum contributions of the coherences. In Fig. 8(b) the signal has also two maxima, although they are almost superposed. This shape is due to the contribution of the $|q|=2$ coherence. For this polarization the complex parts of the tensorial components $\phi^2_{\pm 2}$ of the detection beam have opposite signs so that the contribution of the complex parts of the $\rho^2_{\pm 2}$ coherences [see Fig. 3(b)] do not cancel and originate the two-maxima shape of the $|q|=2$ coherence contribution to the total signal. The hyperfine orientation keeps its contribution unchanged as it is independent of the detection beam polarization.

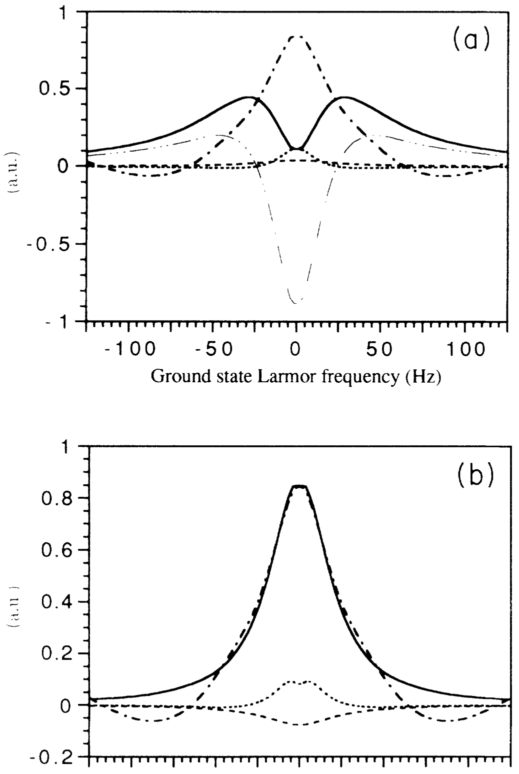

FIG. 8. (a) and (b) Detection signal and contributions of the populations and Zeeman coherences to this signal as a function of the ground-state Larmor frequency. The pumping beam is transversal $\sigma^+$ polarized with uniform spectrum and $W_p=15$. The detection beams are, respectively, transversal $\sigma^+$ polarized and linearly polarized, propagating along the $z$ axis and, with an angle $\theta=54.74°$ between the polarization and the plane determined by the $z$ axis and the propagation direction of the pumping beam. Only the $D_1$ line was used for detection, and $W_d(F_g=3\rightarrow F_e=4)/W_d(F_g=3\rightarrow F_e=3)=0.6$. We plot the total signal (———) and the contributions of the populations, $\rho^0_0$ (—·—·—·) and $\rho^2_0$ (— — —), and of the coherences, $|q|=1$ (— · · · —), $|q|=2$ (· · · ·).

The contribution of a single coherence can be determined experimentally, by combining the profiles obtained for two suitable detection beam polarizations. For instance, the difference between the profile shown in Fig. 8(a) and the one for a transversal $\sigma$-polarized detection beam results to be proportional to the $|q|=1$ coherence contribution. This happens because that contribution is the only one which has the opposite sign when changing in that way the polarization of the detection beam. Another method to detect experimentally the contribution of a single coherence is the one described in Ref. [17], where the atoms in a collimated $^{23}$Na atomic beam are excited with two cw-laser beams. A proper combination of the two consecutive laser beam polarizations allows a selective measurement of the ground-state coherences by means of a polarization-dependent detection of the excited-state emitted fluorescence at the second laser. In Ref. [17] it is shown how the experimental profiles of the total fluorescence signals and in particular those due to a single coherence may present depending on the combination of the polarizations, the one or two maxima shapes similar to the ones that are plotted in Figs. 8(a) and 8(b).

## VI. CONCLUSIONS

In this work we present a complete theoretical study of the relaxation, generation, and detection of multipole orientations in an optically pumped heavy-alkali-metal vapor. It means a generalization of previous partial studies that where limited only to longitudinal components and to particular pumping and detection beam polarizations. Therefore it can be used to model an optical pumping experience for any polarization or spectral distribution of the pumping and the detection beams and it allows us to make clear the dependences on the pumping and detection beam parameters and on the static magnetic-field amplitude of the equilibrium mean values of longitudinal and transversal components and by means of them on the detection profiles. The knowledge of these dependences is especially important for those experiences in cesium in which unbalanced spectrum lamps are used in order to generate stronger atomic polarization or for those experiences in which the quadrupole orientation becomes significant as its presence has been systematically ignored when measuring the parameters that characterize the relaxation of the hyperfine or dipole orientations, which can be the cause of the notable dispersion in their values that can be found in the bibliography. This study is also intended as a basis for further theoretical studies of experiences where the optically pumped atomic system also interacts with external radio or hyperfrequency electromagnetic fields.

[1] W. Happer, Rev. Mod. Phys. **44**, 169 (1972).

[2] E. Bernabeu and J. Tornos, Nuovo Cimento D **5**, 315 (1985); **6**, 261 (1985); **6**, 315 (1985).

[3] J. Tornos and J. C. Amaré, Appl. Spectrosc. **40**, 596 (1986).

[4] A. Omont, J. Phys. (Paris) **26**, 26 (1965).

[5] The terms of the evolution equations associated with the relaxation are denoted by a superscript (c), (s), (d), (sl) (snl), depending on which relaxation process they reflect; respectively, the alkali-atom–buffer-gas collisions, the spin-exchange collisions, the alkali-atom–cell-wall collisions, or the linear and nonlinear parts of the spin-exchange collisions.

[6] F. Grossetete, J. Phys. (Paris) **25**, 383 (1964); **29**, 456 (1968).

[7] W. Franzen, Phys. Rev. **115**, 850 (1959).

[8] F. Masnow-Seeuws and M. A. Bouchiat, J. Phys. (Paris) **28**, 406 (1967).

[9] S. Legowski and P. Rudecki, Bull. Acad. Pol. Sci. Cl. 3 **18**, 43 (1970).

[10] A. Omont, Prog. Quantum Electron. **5**, 69 (1977).

[11] The terms of the evolution equations associated to the pumping process are denoted by a superscript $(p)$ and by a subscript $(a)$, $(b)$, or $(c)$, depending on the stage of the optical pumping cycle that they reflect.

[12] M. I. Dyakonov, Zh. Eksp. Teor. Fiz. **47**, 2213 (1964) [Sov. Phys. JETP **20**, 1484 (1965)].

[13] F. A. Franz and C. E. Sooriamoorthi, Phys. Rev. A **8**, 2390 (1973); **10**, 126 (1974).

[14] M. Rozwadowski and E. Lipworth, J. Chem. Phys. **43**, 2347 (1965).

[15] B. Niewitecka and L. Krause, Can. J. Phys. **54**, 748 (1976).

[16] J. Link, J. Opt. Soc. Am. **56**, 1195 (1966).

[17] R. Schieder and H. Walther, Z. Phys. **270**, 55 (1974).